IOSR Journal of Mechanical and Civil Engineering (IOSR-JMCE)
e-ISSN: 2278-1684,p-ISSN: 2320-334X, Volume 17, Issue 5 Ser. V (Sep. – Oct. 2020), PP 62-74
www.iosrjournals.org

Characterize High Entropy Alloys Thin-Film by an Small Angle X-Ray Diffraction: Review

Asst prof .Dr .Shahin Khameneh Asl[1] Falih Hussein Al-azzawi[2]
1-Department of Materials Engineering, Faculty of Mechanical Engineering, University of Tabriz.
2- Department of Materials Engineering, Faculty of Mechanical Engineering, University of Tabriz.

Abstract
High entropy alloys systems (HEAs) as thin solid films have gained growing attention in recent years. This attention is coming from their tremendous properties such as corrosion resistance, high microhardness, and superior electrical resistivity. These properties, in turn, depend on the structure, chemical composition, imperfection, morphology, and other metallurgical features. Characterizing these features, particularly when approaching from Nano-scale high precision techniques of examination such as X-ray diffraction (XRD), scanning electron microscopy (SEM), scanning probe microscopy(SPM), and X-ray photoelectron spectroscopy(XPS) were adopted. The principle of XRD is based on the elastic coherent scattering for the X-ray monochromatic spectrum with the closest wavelength to the lattice spacing in the crystalline construction. Several geometries are used in the XRD characterize, which leads to different information. THETA -2THETA scan is the conventional and mostly famously mode, where exploited to yield phases patterns with adequate efficiency depends on the lattice planes orientation. For thin-film, large incident angle leads to overlap the peaks of bulk materials with peaks generated by a thin film, for this reason, other techniques were invented.
Keywords *X-ray diffraction (XRD), thin-film, high entropy alloys(HEA), small angle scattering (SAXS).*

I. Introduction

Characterization of the microstructural features of metals, alloys or other materials is a vital activity of metallurgical science. Generally, X-rays diffraction is one of the most important techniques were adopted to probe of crystalline solid materials. it's not only used to reveal the main characteristics of structure like lattice parameter and type of crystal, but the other details such as atomic arrangement in the crystal, imperfection, orientation, grain size, and the size and density of the precipitates[1]. Thin-film characterization and textural measurement can also be performed by X-ray diffraction[2]. X-ray is electromagnetic radiation discovered by chance in 1895 by Wilhelm Rontgen who was interested in working on the cathode-ray (electron beam) developed by the discharge tube, but the wave nature of this ray was conformed in 1913 from the first experiments of diffraction by Max Von Lau [3]. X-rays have a wavelength ranging from 0.1A^o to 100 A^o see figure1. These ranges are equivalent to energies of about 0.1 Kev to 120Kev. Also, Lau showed that the crystalline materials diffracted the X-ray in three dimensional similar to distance separate between their lattice plans. Due to the complexity of three-dimensional model diffraction grating, Bragg can simplify this issue by presenting that diffraction is similar to reflection from different plans of crystal, on condition that certain conditions are met as shown in figure2.The interaction of the imping ray with crystal lead to constructively interference when satisfying Braggs law conditions:

$$n\lambda = 2d\sin\theta \qquad (1)$$

Where: n is a number of wavelength, λ is the wavelength, d interatomic spacing, θ is the diffraction angle.Also, Bragg built their diffractometer to collimate the electromagnetic rays to diffract off of different planes of the crystal. Where the X-rays have been collected in an ionization chamber, then the level of ionization was quantified as a function of the imping angle of the electromagnetic X-rays[1-3].Great efforts have been spent to develop and improve the geometries of the X-ray diffraction inspection method and made it in forefront of non-destructive inspection techniques to characterize complex solid thin – film of high entropy alloys (HEA). High-entropy alloys (HEAs) are comprised of at least five major metal elements, as opposed to traditional alloy systems that are typically based on only one or two major elements. HEAs have attracted attention due to their unique properties such as high strength, good ductility, and high resistance to corrosion and wear [4-5].This review has focused on the use of X-ray diffraction and small-angle geometries to characterize high entropy alloys thin-film

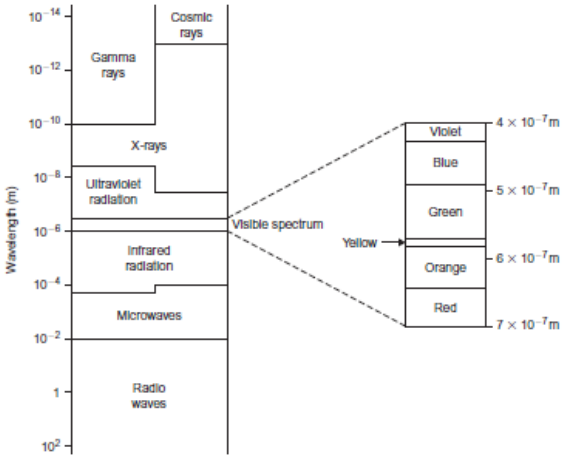

Figure.1: Schematic of electromagnetic radiation[1]

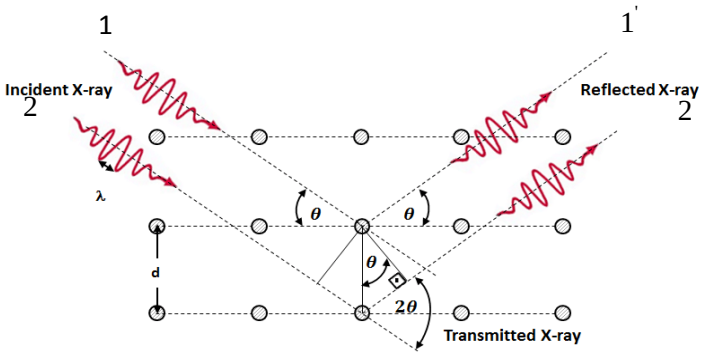

Figure.2: Schematic diagram of Brgg's law [6].

II. Theortical Concepts of X-ray

It is found from Eq.(1) that the Braggs law depends on the wavelength of incident radiation, angle of diffraction and the interplanar distance or plans spacing of crystalline of sample to be analyzed. The diffracted rays are then sensed, treated, and counted, by using 2θ angles range to scan the sample. The scanning should include all probable direction for diffraction occurring of the lattice when inspecting powdered material because it has a random orientation. Translation the peaks of diffraction into d-spacing's help in identifying the compound because each compound has a set of matchless d-spacing. Usually, this is accomplished by comparison of the attained d-spacings with standard patterns cards. About 95% of solids can be characterized as crystalline, and each of them has a unique X-ray "fingerprint", for this, there is a large number of cards represent the fingerprint for different materials used as standard patterns of XRD. Recently about 25000 organic and 50,000 inorganics XRD patterns have been collected and recorded as standard patterns for comparison [7].

Generally-ray diffract meters involve three basic parts: an X-ray tube, a sample holder, and an X-ray detector [8]. X-rays are the electromagnetic form of radiation different from the light and the has a shorter wavelength about (λ=0.1nm) produced from the target of metal (anode) may be from (tungsten, molybdenum, copper, Iron, or Chrome) is bombarded by the accelerated beam of electrons emitted from the cathode in the air vacuumed tube under high drop voltage for example 30- 150 Kv (Figure.3a). The emitted ray (Figure.3b) is divided into two parts, the continuous or white rays that are spread over an extended range of wavelengths, the second part or component it's the line spectrum(characteristic spectrum), which represents the feature of the bombarded material. "White" radiation, resulting from the collision between the bombarded electrons and the target electrons. The lowest wavelength (λ_{min}) happens in the white spectrum which is identical to the total energy of an electron that it loses in one single collision. i.e.$\left(\lambda_{min} = \frac{h_c}{ev} = 12.4 \times 10^3 V^{-1}\right)$ [1].

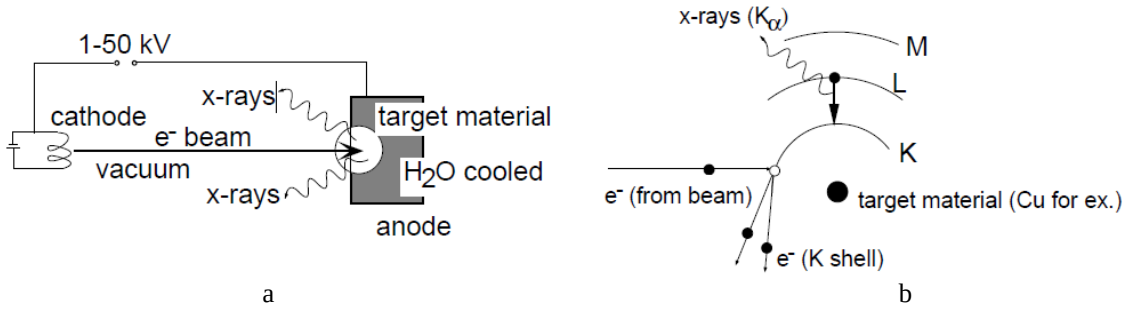

a b

Figure.3: Schematic of X-ray generation [8].

The intensity of the white spectrum is depended on the target metal atomic number Z and almost on the square of the utilized voltage. The line spectrum initiates just when the critical voltage is exceeded and this occurred as the accelerated electrons pose adequate energy to dislodge the internal electrons from its shell (for instance1s-level), this ejecting process creates vacant in 1s- a level which is filled by an electron coming from a higher energy shell, x-ray emission occurs through the electrons transition. If this electron moves from the adjacent second L- shell . in this case the emitted radiation is called K- alpha radiation (Kα)There are two components of Kα is Kα1 and Kα2. Equation (2) used to calculate the wavelength.

$$h_v = E_L - E_K \qquad (2)$$

But if the electron transmitted from M-shell to fill the vacancy, K-beta radiation(Kβ) is emitted(Figure.3a). it is worth noting that these two radiation components are originally inseparable so that it cannot radiate one of them without the other. For this, the characteristic or line K- radiation radiated from a copper target is encompassed of an intense Kα- radiation besides Kβ-radiation where it is weak. Copper is widely used as a target material for single crystal diffraction with Kα radiation = 1.5418 Angstrom. Table 1 indicates the metals used as a target in an X-ray source. Losing intensity of X-ray bean can calculate from during electron transmitting process Eq.(3) [2].

$$I = I_O \times \exp^{[-\mu x]} \qquad (3)$$

Where I, Io: are the initialand final intensities. μ: is a coefficient of linear deposition and depends on the x-ray wavelength and the absorber nature. X referred to the thickness of the target. some aspect must be defined such as mass absorption constant i.e. (μ/ρ) where ρ is a density, critical wavelength value λ_k it is the value of wavelength at which the absorption decreases drastically and called K-absorption edge it is characteristic of the absorbing metal (Fig.3b), which X-rays have adequate energy to dislodge the electron from K-shell, and similar for L and M edges happen at larger wavelength. Unwanted radiation components like Kβ-radiation and short wavelength of the white spectrum should be filtered out. Filtration process achieved by putting a small thickness piece of Nickel in a path the beam of X-ray. This filter will only be allowed to Kα-radiation to pass through it. Radiation extracted from the filtering process is adequately monochromatic for several X-ray techniques; hence, crystal monochromators from quartz or lithium fluoride are used to reflect the desired wavelength according to Brags law. When a monochromatic X-rays spectrum directed into an atom, the electron around the atom is started to oscillate with the same frequency of the incident beam. The sample to be scanned should be rotated in a different direction to avoid destructive interference, which occurred when combining of waves external of phase and no leaving of energy from the scanned specimen. The detector can also rotate around the sample with a doubled angle of (θ) in certain angular velocity to record the reflected X-rays intensity (Fig.4). Constructive interference occurs and a peak of diffracted X-rays recorded by the detector if the geometry of the directed X-rays that collides the sample satisfy Braggs law. Then the signal is processed and converted into a count rate and then output [1].

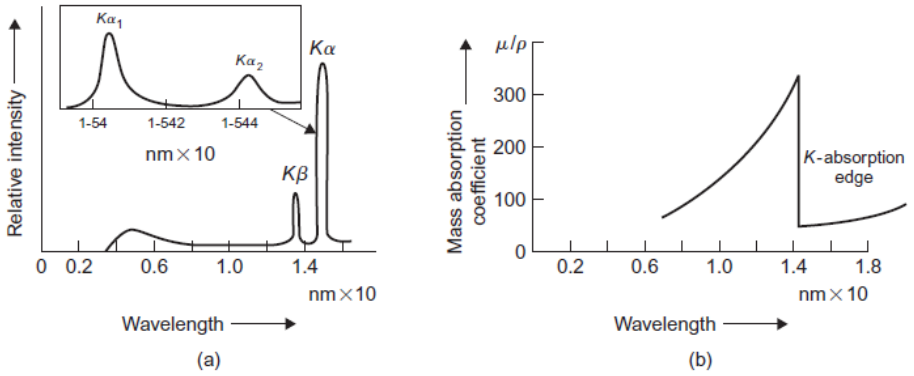

Fig.4. (a) Intensity of X-ray from Cu target (b) K- absorption edge on X-ray wavelength for Ni [1].

Table1: target metals with k-radiations components and filters [9].

Target	$K_{\alpha 1}$	$K_{\alpha 2}$	$K_{\alpha \text{ mean}}$	K_{β}	Excitation potential	Filter
Cr	0.22897263	0.22936513	0.22910346	0.20848881	5.98	V
Mn	0.21018543	0.21058223	0.21031770	0.19102164	6.54	Cr
Fe	0.19360413	0.19399733	0.19373520	0.17566055	7.11	Mn
Co	0.17889961	0.17928351	0.17902758	0.16208263	7.71	Fe
Ni	0.16579301	0.16617561	0.16592054	0.15001523	8.33	Co
Cu	0.15405929	0.15444274	0.15418711	0.13922346	8.98	Ni
Mo	0.07093000	0.07135900	0.07107300	0.06322880	20.0	Zr

III. Theoretical consideration of XRD

XRD is an analytical method investigating the scattering of X-ray from the crystalline of the solid materials. Every material has a matchless X-ray "fingerprint" of the X-ray intensity vs. angle of scattering which is characterized by its atomic structure. The solid material can be categorized as Amorphous, which has a random arrangement of its atoms as the same as disordering in liquid. Glass is classified as amorphous materials, and crystalline materials, which have regular atomic structure, and are built from very small volume unit cell which is periodically repeated in three dimensions, describe the crystal. Three coordinates (a, b, c) and three angles between these (α, β, γ) are used to describe the dimensions for the unit cell.When the interference is constructive, a diffracted beam from crystal may be designed as a beam included a large number of scattered radiations mutually support each other. For simplicity, the reflection from a parallel plane inside the crystal is the best analytical method. The direction and the interplanar distance or spacing between these planes are described by three integers (h, k, l) known Miller indices (Fig.5). Also, they represent the intersection values with axes of the unit cell [10].

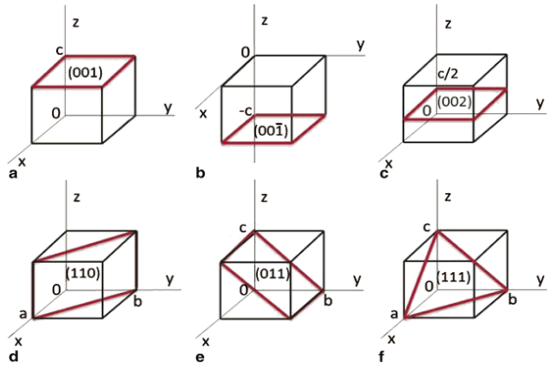

Fig.5. Miller indices [10]

From Fig.1 and miller indexes it can rewrite the Bragg's law as follow for symmetrical simple cubic crystal when the size of the unit cell, the diffraction angles of the diffracted beam from the crystal planes (hkl) can easily be found or calculated from the interplanar distance relations.

$$d_{(hkl)} = {}^{a}/_{\sqrt{(h^2+k^2+l^2)}} \ldots\ldots\ldots 3$$

$$\lambda = \frac{2a \sin\theta}{\sqrt{(n^2h^2+n^2k^2+n^2l^2)}}$$

$$\lambda = 2a \sin\theta/\sqrt{N} \ldots\ldots\ldots\ldots\ldots\ldots\ldots 4$$

Where n is the order of reelection, N is known as reflection or line number. For example the 2nd order reflection from plane (100) of iron – α (bcc). Then, since n=2, h=1, k=0, l=0, this type of reflection is indicate to either the reflection from plane (200) or as line 4 see figure 6. the planes that lead to a reflection at the smallest Bagg's angle are those which have most widely spaced, i.e. they are the lattice which interplanar spacing equal the full scale axis of unit cell, d_{100}=a, in this case ($a = \frac{\lambda}{2 \sin\theta}$) and display small diffraction peak. Though, electrons distribution inside the unit cell is determined the reflection intensities. Electron density increases around atoms. For this, planes that going through the zones have high electron density give strongly reflecting, planes which have low electron density exhibit weak intensities [12].

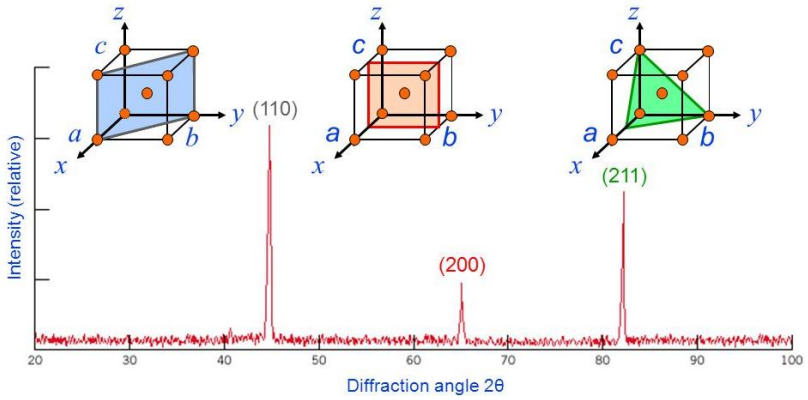

Fig.6. XRD patterns of α-iron (bcc) [13]

XRD Goniometer Essential

A goniometer is the precision mechanical instrument that has two axes (ω and 2θ) used either to measure the angles or permits to equipment assembled such as (sample holder, and detector arm) with it to be moved with a precise angular motion to measure X-ray intensity. Where the sample holder is setting on the ω-axis and the detectors are set on the 2θ axis [14]. Fig.6 shows the Bragg-Brentano part focusing on goniometer. The distance between the focal spot of monochromatic X-ray bean and the center of the holder (or sample) similar to the distance between the detector and sample. Where if there is any relative motion between the sample and the detector, the diffracted radiation will stay focused on the constant radius circle. There are two types of Bragg-Brentano part focusing goniometer is THETA: 2-THETA goniometer in which the holder of sample moves by the angle θ and the detector concurrently moves by the angle 2θ. Usually, his type is relatively suitable for a big sample. The other type is THETA: THETA goniometer in which the sample is in horizontal position and both of the X-ray source and detector move over the angular range of θ simultaneously. To reduce an angular dispersion and to enhance the spatial resolution for the collided and the diffracted beam, some slit is placed in the path of the x-rays beam [11, 14].

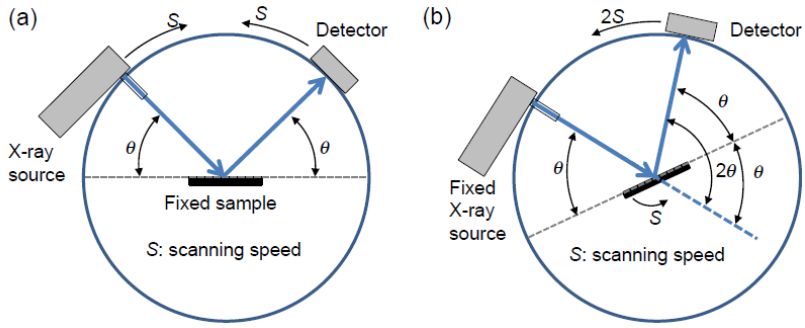

Figure.6: Schematic shows the types of XRD Goniometers, (a) θ-θ type, (b) θ- 2θ type [14]

IV. X-ray Diffraction Methods

Primarily, there are two methods were used to generate an XRD.

4.1 Single Crystal or (Laue) Method

In this method, a small single crystal of material with a fraction of millimeter in size is fixed in the path of the "white" X-rays beam. The essential parameter to confirm that Bragg's law is achieved for all the planes inside the crystal should be provided by the range of wavelengths in the beam. Usually, X-rays sources with higher atomic number targets (tungsten) are used to generate a "white" spectrum, or any source generate "white" radiation is suitable. The diffracted spectra may be revealed as a transmission photograph or a back reflection photograph (Fig.7). Both appearances depend on the relative sits of the X-rays source, crystal, and detector or film. Where, in the transmission case the crystal is located between source and film, in this state the produced spots create ellipse profile but in the back-reflection case the film is the medium between crystal and the source of "white" beam, in this state generated spots produced hyperbolic profile. The Laue method is widely used to determine the single crystals. Essentially, the determination process is based on the plotting the regions taken from the photograph onto a stereogram, after that comparing process of the angles is carried out between them and standard charts which is contained the projections of that crystal structure. Recently, the Laue method used to determine the crystal distortion because it is found that the spots from perfect single crystal are sharp, but those created by deforming crystal are elongated. The elongated semblance of the spot's reflection is called Asterism [1, 11].

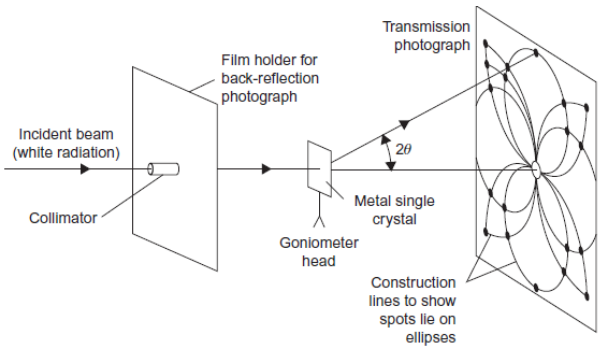

Figure.7: Schematic shows Laue method [1].

4.2 Powder Method

This method is firstly discovered by Debye and Scherrer, almost it can be considered the most used method of all XRD techniques. In this method monochromatic X-rays source and a finely grain polycrystalline powder, wire specimen. In this technique, θ, is the essential variable, since the sample is a set of randomly oriented crystals, therefore it binds sufficient numbers of particles with correct direction to permit reflection from each of the possible reflecting planes. 2θ represents the angle between the monochromatic beam and the diffracted radiation, based on that each set of planes in the crystal leads to a cone profile of reflected rays of similar angle 2θ, θ is the Bragg's angle for that specific set of reflecting planes giving the cone. Thus, if a film is fixed around the sample (Fig.8), the successive reflected cones, which include spectra from hundreds of grains, cross the film to generate concentric curves around the entrance and exit holes. Figure 8 illustrates examples of patterns from bcc and fcc materials, respectively. Accurate measurement of the pattern of diffraction lines is essential for several applications of the Debye-Scherrer method**.** The lines incident on the photograph film have spotty appearance. Occasionally, this behavior is used as a tool to determine the size of grain of a polycrystalline specimen. There are series of photograph pattern of known grain size used as a standard in the comparison

process. preferred direction of the grains of polycrystalline aggregate can also be detected by Debye-Scherrer technique. Due to the completely randomized direction of the grains of the powder sample create a complete Debye –ring, whereas a favored orientation, texture, or if there are just a few crystals the appearance will be incomplete Debye-ring [1,15].

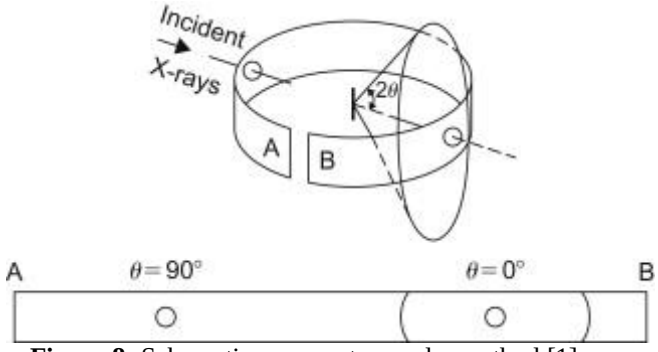

Figure.8: Schematic represents powder method [1].

V. Special XRD Techniques

Several techniques were developed to analysis thin solid film such as energy dispersive X-ray diffraction (EDX), In situ X-ray diffraction (IXD), small angle scattering (SAXS). This review will be limited to using both XRD and SAXS in the analysis of thin-film.

5.1. Small Angle X-ray Scattering (SAXS) Technique

Small-angle was firstly observed by Guinier (1937), then, Peter Debye, Otto Kratky, and others which are developed the theoretical and experimental principles of this strategy, but the huge progress in refining this technique started in the 1970 and is continuing today, as a result of the increasing demand to study the properties of the substance within the limits of the Nano-scale [16, 17]. SAXS is one of the most important analytical techniques of X-ray scattering family. It is an effective analytical tool used to make known information about the structure, crystallography, heterogeneity, chemical composition, physical properties, and thin films, where it is widely adopted by global scientists since the 1950s[18]. This technique is dependent on detecting the intensity of a narrow wavelength elastic scattering of a monochromatic X-ray spectrum impinging a sample at a very low range of scattering angle. When X-ray radiation passes through the sample it causes electrons to vibrate to the same frequency of the impinging wave, These vibrating electrons lead to generating coherent secondary electromagnetic waves that have the same wavelength as that of the impinged waves. Any scattering process is defined by a reciprocity law which represents an inverse relationship between target size and angle of scattering. Based on this theory, the vector of wave transfer (q) is computed based on the intensity of scattering and the scattering vector, as presented in Eq. (5). Fig. 9 shows the incident beam of SAXS [19].

$$q = \frac{4\pi \sin\theta}{\lambda} \dots\dots\dots\dots\dots\dots (5)$$

where θ is the incidence angle and λ is the wavelength of an incident radiation [20]

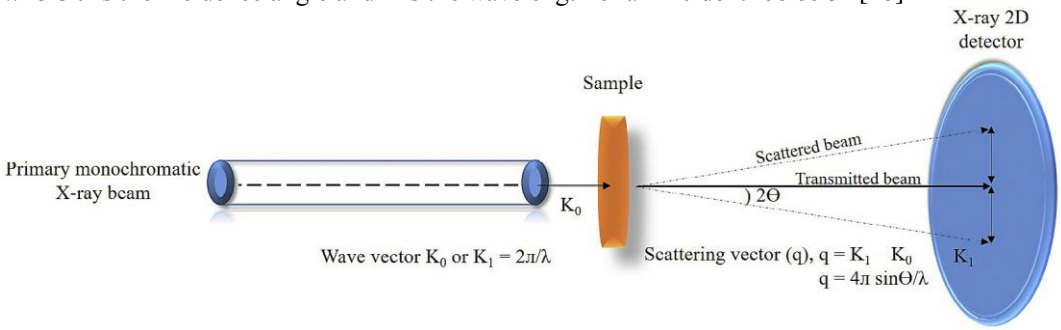

Figure.9: Schematic diagram shows SAXS technique [20].

Initially, several hours were spent to get one useful profile of the scattering for a spacemen [21], but the time is reduced to less than 10ms due to significantly development of the technique of X-ray and synchrotron radiation sources [22].

5.2 SAXS Theoretical Concepts

The scattering X-ray intensity at a small angle zone ($2\theta = 0.1^{o}$ to 10^{o}) establishes from the existence of the in homogeneities or imperfections in the structure of the substance to be examined (for example a small cluster of solute atoms), whereas, these in homogeneities possess dimensions only 10-100 times the wavelength of the monochromatic incident beam. Essentially, the scattering of X-ray has resulted from the difference in the electron density among heterogeneous zones and the material matrix that it's surrounding. For this, the precipitated particles represent the major sources of diffraction. Other imperfections like dislocations, vacancies, and cavities also initiate some SAXS, but the intensity of diffracted radiations is much weaker than that those of precipitates or second phase particles. Generally, the measurement process is achieved in transmission with fine-focused monochromatic X-rays spectrum at the thin specimen, with diffraction angles have range lower than 10o, and using the two-dimension detector in measurement. however, in the SAXS crystal planes don't take into consideration for diffracting monochromatic X-rays beam, instead of that, a small constituent within the substantial such as fibers, second phase particles, precipitate, etc. the presence of these constituents lead to irregular electron distribution especially at the boundaries of inspected structures, which in turn larger deflection of the collimated spectrum[1,23]. Consequently, this method is typically helpful in collecting information on structures with dimension limits between 5 and 150 nm [24]. This phenomenon is firstly studied by Ander Guinier derived approximation relationship to interpret the large number of SAXS data [19].

$$I = Mn^2 I_e e^{[-4\pi^2\varepsilon^2 R^2/3\lambda^2]} \dots\dots\dots\dots\dots 7$$

Where M indicates to the number of scattering aggregates, or particles, in the spacemen, n specifies to the difference in electrons number between the particles and an equal volume of the surrounding matrix, R is the particle radius of gyration, I_e scattered intensity is the scattering angle, λ is the X-ray wavelength. Equation 7 refers that the intensity of SAXS is zero when the heterogeneities have the density of electron equivalent to the boundaries, even if it possesses quite different crystal structures. From plotting the relation between log10 I as a function for $\varepsilon 2$ the slope nears the origin, $\varepsilon=0$, is given by:

$$P = -(4\pi^2/3\lambda^2)R^2 \log_{10} e \dots\dots\dots.8$$

For Cu-kα- radiation $R = 0.0645 \times P^{1/2} \dots\dots\dots\dots\dots.9$

Low angle range (almost close 0^{o}) and very small cohesion scattering of X-ray may be (wavelength 0.1……0.2nm) made SAXS is an ideal technique for experimenting regions of structure which have a scale of segregation to be discernible by the light microscope, for example (earlier stages of phase precipitation, and the lattice defects aggregations) [1, 19].

5.3. X-Ray Source and Optics for SAXS

In 2D- SAXS system the scattered X-rays are gaged in all 360∘ azimuthal angles at the same time. Thus, the X-ray source and optics imposes versatile optical specification to meet with requirements of SAXS. the X-ray spectrum required for SAXS should have long beam path, low divergence, and small beam size. Any of conventionally used target metal, like Cu, Co, Cr can be adopted for SAXS, but Cu-Kα radiation is preferred because it is not suffering from absorption as that in the Cr-Kαradiation which has a longer wavelength. Another importance in the target election is preventing fluorescence. Due to the small angles of scattering, the scattering pattern from the Kα1 and Kα2 components are continuously merged. The monochromatization by crystals of graphite or multilayer mirrors can produce appropriate spectrum purity. Collimation is the most crucial part of a SAXS system. The collimation part describes the size, shape, and divergence of the X-ray beam (separate the weak component from the strong component in the X-ray primary beam) [25]. Collimation also limits the resolution of a SAXS system.Fig11 illustrates the collimation part of the SAXS system with a pinhole collimator, sample, beam stop, and detector. The job of the beam stop is to make the incoming beam from striking the detector. The scattering from the material of the second pinhole leads to pinhole scattering also known parasitic scattering, this scattering is as a halo around the shadow of the beam stop. The third pinhole in the (Fig.10a) used as anti-scattering to limit the region of parasitic scattering. Parasitic scattering by slits or pinholes is a dangerous issue for SAXS, which consequences in high background and undesirable artifacts to the image as well as lower resolution limit as a result to the large beamstop. Using scatterless pinholes can drastically overcome the problem (Fig.10b). The collimation with two scatterless pinholes helps shrink the length of system, eliminate most of the parasitic scattering, and expand the resolution limit with smaller beamstop[26].

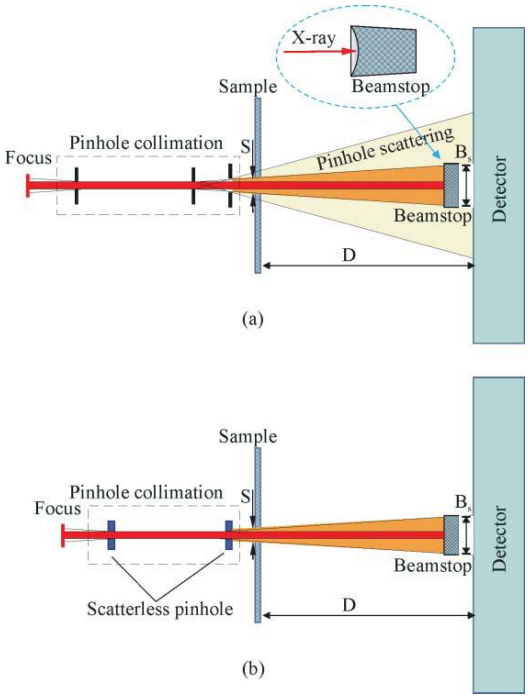

Figure.11: Pinhole collimation for SAXS: (a) conventional collimation with three pinholes, (b) collimation[19].

5.4. SAXS System

Two-dimensions XRD devices that used for wide-angle X-ray scattering(WAXS) utilized in two dimension SAXS data collection, relating to the wanted resolution and quality of data. X-rays spectra size and parallelism, as well as detector resolution, determine the SAXS angular resolution. For this, the distance between the first and the second pinholes should be increased to give rise to high parallelism and decrease the collimator parasitic scattering. the high intensity of scattering and the tailing part of the incoming beam close the beam stop edge, and fast weakening of scattering intensity with the scattering angle, the area detector for two-dimensional SAXS should have appropriately dynamic range to simultaneously achieve the high counts near the beam stop and low counts of high order features. another prerequisite of 2D SAXS detectors is a high spatial resolution. Precise scattering patterns details can be obtained by SAXS system with a high angular resolution which in turn achieved when the degree of the spatial resolution of the detector is high, the path length of the secondary beam is long, and small size of X-ray beam(Fig. 11). Typically, 2D- detectors used to collect SAXS data, it can reveal anisotropic characteristics from samples to be examined(polymers, fibrous or layered materials, single crystals, and biomaterials). It is be noted, The 2D detector is the most important part of a dedicated SAXS system[19,27].

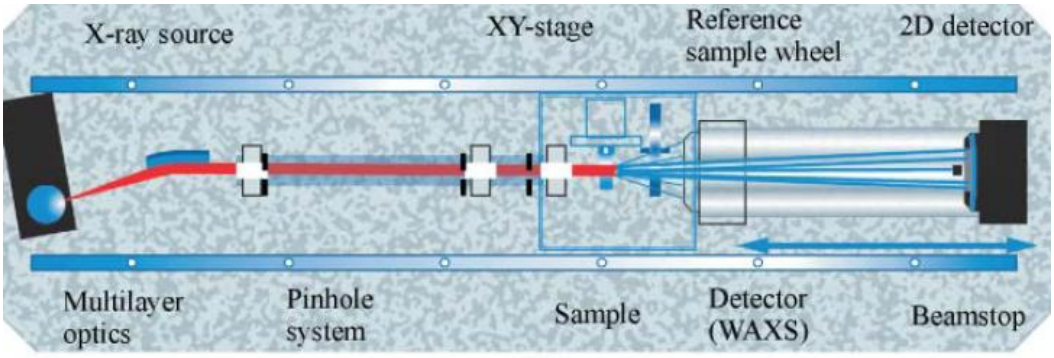

Figure.11: Schematic diagrams show the side view of SAXS system [27].

The third pinhole in the schematic diagram work as an anti-scatter pinhole. large distance between the first and second pinholes work on parallelism achievement and minimizing the parasitic scattering by lowering the beam divergent. The XY stage used to fix the specimen several specimens can be loaded in the chamber at the same time. Usually, The specimen chamber and secondary and primary paths of the SAXS system have been evacuated together. in some cases chamber can be separated from the path, in this case, it is filled with other gas

environments or pressurized. The secondary module beam path system allows various specimen-to-detectors distances, for example, 650–2000mm for SAXS, or as close as the sample chamber for wax. A 2θ of 40◦ can be measured with either an MWPC Hi-Star™ or a Mikrogap V◗ntec-2000™ detector in a WAXS configuration. The primary beamstop is made of metal that has high absorption and less fluorescence, such as gold, tantalum, tungsten, or Pb-Sb alloy. The size of the beamstop is chosen according to the size of the beam and divergence [19].

VI. XRD and SAXS applications

The conventional XRD and scattering are applied in the sub-domain of the wide-angle X-ray scattering(WAXS)[28]. the patterns of scattering in the wide-angle field reveal information on the polymer chain segment arrangement. Also, studied the orientation variation of the chains of the amorphous phase, unit cell structure, crystal size, distortion of crystal and crystalline. usually, SAXS region used to study the structure in the micro scale or Nano-scale for the particle regimes(solid, liquid, solid-liquid systems, and colloidal systems), the structure, orientation, and distortion of ordered of lamellae stack, the structure of semi-crystal substances, thermoplastic elastomers, copolymers multi-phase blends, crazing. application extending to include metals, cement, oil, proteins, food, and pharmaceuticals[29,30,31]. this review highlights the use of XRD and SAXS techniques for thin-film characterization.

AKito Sasaki [32], exploited the SAXS method to determine the distribution density of different Nano-particles. SAXS examinations were achieved in both the transmission geometry to measure dispersed of particles in solvent or bulk films, and the geometry of reflection to quantify dispersed of particles in thin films deposited on substrates. The results showed, there is an agreement between the X-ray distribution density examinations with outcomes of tunneling electron microscopy(TEM) experiments. Also, estimated the size distribution of sub-Nano-cluster by TEM is not possible, but successfully performed by SAXS.V. **Thomann et al**.[33] characterized the thermal stability of two AlCoCrCuFeNi HEAs thin-film magnetron sputtering by the in the situ-XRD method. HEA is an alloying system that includes five to thirteen principle elements, with equiatomic or different concentration mixing, to exhibit interesting properties. high entropy mixing maybe leads to the formation of one or more of the solid solution with Nano-crystalline or amorphous structure. XRD characterization conducted(Brucker D8) diffractometer using the Cu-Kα spectrum X-ray source and with a scanning speed of 40 °Cmin−1 before and during post heat treatment(annealing). The results showed there is no change in the phase stability until 510oC annealing temperature for two samples, but they are exhibit different behavior at high temperatures (Fig.12).

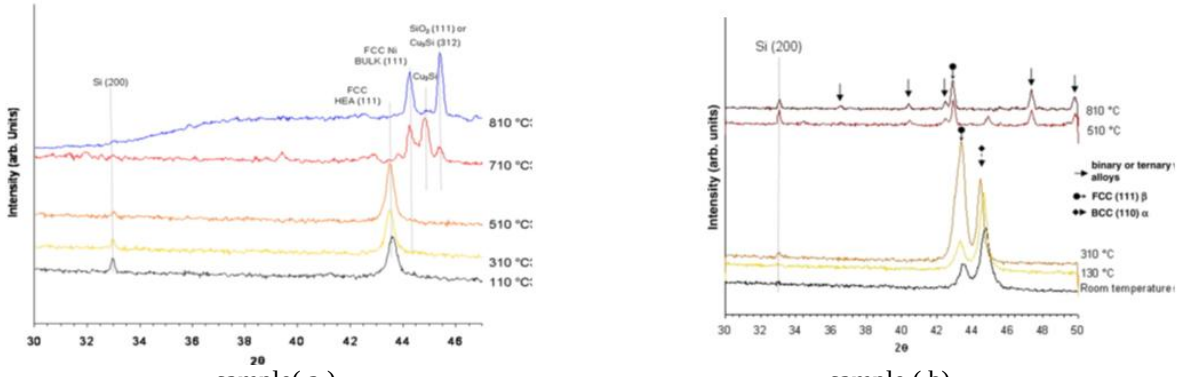

sample(a) sample (b)

Figure.12: XRD patterns of two samples evaluate their behavior during annealing.

R. KAMIYA et al.[34], used *(2D-GIXD)* to characterize the crystal structure of TIPS-pentacene thin films are synthesized by wet and dry processes on the SiO2/Siwafers. **Koundinya et al.[35],** used Rigaku Ultima-III x-ray diffractometer with Cu- Kαr spectrum (1.5406 A˚) at a scan step of 0.02o to analyze the progress of phase formation in an equimolar nanocrystalline AlCrCuFeNiZn HEA during milling process for a different milling time. The XRD patterns indicate the reduction in peak intensity of phase and element with milling time. This behavior can be attributed to mutual diffusion of the element to form a solid solution. **A. Narayanan and Konovalov[36],** X-ray scattering techniques are desired for the structural investigation of these materials both in bulk and at the interfaces. The scattering contrast originates from the spatial fluctuations of the electron density that systematically differs with the number of atomic of constituent elements. SAXS delivers a structural resolution of the order of 1–100 nm for investigations in the bulk. Zhinan et al.[37], synthesized single-phase solid solution a thin – film from the CrCoCuFeNi HEA via Rf –magnetron sputtering deposition process. approximately, all the five elements in HEAs have quite similar scattering factors

to any energy of photon which is out of range of their absorption edges. Though, some ordered structures or second phases like FeNi3 may not be visible by the conventional XRD technique. For this, high-energy synchrotron X-ray with transmission diffraction with (with the 115keV incident beam energy at the beamline of 11-ID-C at advanced photon source(APS)) used for the substrate, and grazing incident X-ray scattering (GIXS) accomplished with the 20 keV incident beam energy and 0.5o grazing angle at the line of beam 33-BM, to confirm the solid solution in thin films . **Marshal et al [38],** grown thin-film from FeMnCoCrAl high entropy alloy on the Si substrate by DC magnetron sputtering in an inert gas of Ar(3torr). Also, another sample with the same concentration was prepared from FeMnCoCrAl pure powder as –cast by arc melting to ascertain the probable difference in the formed phases and properties between the HEA thin- film and the substrate. The crystal structure of the thin layer and substrate were characterized by Siemens D5000 XRD diffractometer with monochromatic Cu- Kα spectrum X-ray source. Bruker D8detector was used to record an XRD pattern in the incidence of a grazing angle(10^o)**. Chao et al.[39],** used XRD diffractometer to characterize the structure of AlxCoCrFeNi (x =0.3, 0.6 and 0.85) HEA layer, which deposited by direct laser on the stainless steel substrate and how to affect the x fraction, process parameters, and isothermal process on the structure and mechanical behavior of deposited layer. XRD characterization showed the existence of ordered BCC phase (B2) with a very minor (100) peak after isothermal annealing for 100h at 1000^oC. **Ioana Csaki et al.[40**], presented an experimental study to evaluate the phases and analysis of the microstructure of CoCrFeNiMo high-entropy alloy(HEA) for electro spark deposited coatings for the geothermal environment.). Emission Scanning electron microscope (SEM) coupled with energy-dispersive spectroscopy (EDS), and X-ray diffraction (XRD), used to analyze the microstructure, morphology and chemical composition of the coating layer. The (Co Cr Fe NiMo) deposited layer crystal structure was FCC identified by the XRD test, BCC structure, and potential σ phase also was formed for (Co Cr Fe Ni Mo). Huang et al.[41], used the SAXS method to evaluate the effect of aging time on the kinetics growth of nano –precipitates(ppts) of the severe cold- deformed CoCrFeMnNi HEAs which aged at 350-500oC for various times. the sample prepared as cast by melting the mixed powder s of CoCrFeMnNi with 99.9wt% purity in vacuum arc furnace then molded for proper shape, after that the ingot cold- deformed by rolling to reduce the thickness to about 85%. Samples homogenized at 1200oC for 24h. SAXS specimens cut in10x10 mm2 with 20μm thickness then loaded to the evacuated quartz tube foraging for different times. The SAXS examinations were carried out at the BL23A beamline, National Synchrotron Radiation Research Center(NSRRC), Taiwan, with high-flux collimated X-rays of 15 keV and a ~500 μm size of the beam. each 2D SAXS pattern was azimuthally averaged into a 1D SAXS profile as a function of the scattering vector($Q=4\pi\sin(\theta/2)/\lambda$), where θ is the scattering angle. Results showed there is drastically in the ppts during the early 30min at aging temperature 500 °C until 60min were reaching saturation aging.

VII. Conclusions

Several physical aspects have been reviewed in this review can be summarize as:

1. X-ray diffraction fundamentals, X-ray generation, X-ray spectra types, Bragg's law, diffraction methods (single crystal, and powder methods) both methods are based on elastic coherent of X-rays scattering due to interact with atomic electron of crystalline substance.
2. X-ray diffraction instrumentations. Two types of goniometer also have been discussed like theta –theta, and theta -2theta types.
3- characterization thin film with nano- scale thickness, and material heterogeneities with 10 to100 time of incident wavelength, by conventional XRD technique, show it is inability to identify these geometries. For this, special advanced techniques based on scattering were developed such as energy dispersive X-ray diffraction (EDX), In situ X-ray diffraction(IXD), small angle scattering (SAXS) to perform the characterize these geometries.
4. this paper also reviewed some efforts that used both of SAXS and XRD in characterize high entropy thin film.

References

[1]. Smallman, R. E., and A. H. W. Ngan. "Modern Physical Metallurgy (Eight Edition)." Chapter 5 (2014): 219. Brindley, G. W., and G. Brown. "Quantitative X-ray mineral analysis of clays." Crystal structures of clay minerals and their X-ray identification 5 (1980): 411-438.

[2]. Bunaciu, Andrei A., Elena Gabriela UdriŞTioiu, and Hassan Y. Aboul-Enein. "X-ray diffraction: instrumentation and applications." Critical reviews in analytical chemistry 45.4 (2015): 289-299.

[3]. Guinebretière, René. X-ray diffraction by polycrystalline materials. John Wiley & Sons, 2013.

[4]. Lutterotti, Luca. "Total pattern fitting for the combined size–strain–stress–texture determination in thin film diffraction." Nuclear Instruments and Methods in Physics Research Section B: Beam Interactions with Materials and Atoms 268.3-4 (2010): 334-340.

[5]. Tsai, Ming-Hung, and Jien-Wei Yeh. "High-entropy alloys: a critical review." Materials Research Letters 2.3 (2014): 107-123.

[6]. Sowinska, Malgorzata. "In-operando hard X-ray photoelectron spectroscopy study on the resistive switching physics of HfO2-based RRAM." (2014).

[7]. Sharma, Ravi, et al. "X-ray diffraction: a powerful method of characterizing nanomaterials." Recent Research in Science and Technology 4.8 (2012).

[8]. Connolly, James R. "Introduction to X-ray powder diffraction." Diffraction Basics II: Intensities ", EPS400-001, epswww. unm. edu/xrd/xrdclass/06-Diffraction-Basics-II. ppt (2007).

[9]. Epp, J. "X-ray diffraction (XRD) techniques for materials characterization." Materials characterization using Nondestructive Evaluation (NDE) methods. Woodhead Publishing, 2016. 81-124.

[10]. Tilley, Richard JD, and R. J. D. Tilley. Understanding solids: the science of materials. Hoboken: Wiley, 2013.

[11]. Wang, Gwo-Ching, and Toh-Ming Lu. "Crystal Lattices and Reciprocal Lattices." RHEED Transmission Mode and Pole Figures. Springer, New York, NY, 2014. 7-22.

[12]. Larsen, Finn Krebs, and Niels Kristian Hansen. "Diffraction study of the electron density distribution in beryllium metal." Acta Crystallographica Section B: Structural Science 40.3 (1984): 169-179.

[13]. Waseda, Yoshio, Eiichiro Matsubara, and Kozo Shinoda. X-ray diffraction crystallography: introduction, examples and solved problems. Springer Science & Business Media, 2011.

[14]. Epp, J. "X-ray diffraction (XRD) techniques for materials characterization." Materials characterization using Nondestructive Evaluation (NDE) methods. Woodhead Publishing, 2016. 81-124.

[15]. Hargittai, István. "Christopher Hammond: The basics of crystallography and diffraction." (2009): 751-751.

[16]. Glatter, Otto, and Otto Kratky, eds. Small angle X-ray scattering. Academic press, 1982.

[17]. He, Bob B. Two-dimensional X-ray diffraction. Vol. 2. Hoboken: Wiley, 2009.

[18]. T. Nousiainen, E. Zubko, H. Lindqvist, M. Kahnert, J. Tyynela, Comparison of scattering by different nonspherical, wavelength-scale particles, J. Quant. Spectrosc. Radiat. Transf. 113 (2012) 2391e2405.

[19]. He, Bob B. Two-dimensional X-ray diffraction. Vol. 2. Hoboken: Wiley, 2009.

[20]. Li, Jingpeng, et al. "Application of the small-angle x-ray scattering technique for structural analysis studies: A review." Journal of Molecular Structure 1165 (2018): 391-400.

[21]. L. Boldon, F. Laliberte, L. Liu, Review of the fundamental theories behind smallangle X-ray scattering, molecular dynamics simulations, and relevant integrated application, Nano Rev. 6 (2015) 25661.

[22]. J.-r. Huang, L.R. Warner, C. Sanchez, F. Gabel, T. Madl, C.D. Mackereth,M. Sattler, M. Blackledge, Transient electrostatic interactions dominate theconformational equilibrium sampled by multidomain splicing factor U2AF65:a combined NMR and SAXS study, J. Am. Chem. Soc. 136 (2014) 7068e7076.

[23]. Epp, J. "X-ray diffraction (XRD) techniques for materials characterization." Materials characterization using Nondestructive Evaluation (NDE) methods. Woodhead Publishing, 2016. 81-124.

[24]. Axel Knutsson (2008) structural characterization of Arc evaporated TiAl/TiN multilayers

[25]. Vaughan GB, Wright JP, Bytchkov A, et al. X-ray transfocators: focusing devices based on compound refractive lenses. J Synchrotron Radiat. 2011;18(Pt 2):125–133. doi:10.1107/S0909049510044365.

[26]. Incoatec Product Flyer, SCATEX – Scatterless pinholes for home-lab systems, IDO-F20-005A (2015), Incoatec GmbH, www.incoatec.de.

[27]. J. S. Pedersen, A flux- and background-optimized version of the Nanostar small-angle X-ray scatteringcamera for solution scattering, J. Appl. Cryst. (2004). **37**, 369–380.

[28]. P. Boesecke, Reduction of two-dimensional small- andwide-angleX-ray scattering data, J. Appl. Cryst. (2007). **40** (Supplement), s423–427.

[29]. Zeinolebadi, Ahmad. In-situ Small-Angle X-ray Scattering Investigation of Transient Nanostructure of Multi-phase Polymer Materials Under Mechanical Deformation. Springer Science & Business Media, 2013.

[30]. https://en.wikipedia.org/wiki/Small-angle_X-ray_scattering

[31]. Narayanan, Theyencheri, et al. "A multipurpose instrument for time-resolved ultra-small-angle and coherent X-ray scattering." Journal of applied crystallography 51.6 (2018): 1511-1524.

[32]. Sasaki, Akito. "Size distribution analysis of nanoparticles using small angle X-ray scattering technique." Rigaku J 22.1 (2005): 31-38.

[33]. Thomann, Anne-Lise, et al. "Thermal stability and in-situ XRD analysis of AlCoCrCuFeNi high entropy alloy thin films." 2009.

[34]. Kamiya, R., et al. "Two Dimensional Grazing Incidence X-Ray Diffraction of TIPS-Pentacene Thin Films." Molecular Crystals and Liquid Crystals 568.1 (2012): 134-138.

[35]. Koundinya, N. T. B. N., et al. "Phase evolution and thermal analysis of nanocrystalline AlCrCuFeNiZn high entropy alloy produced by mechanical alloying." Journal of materials engineering and performance 22.10 (2013): 3077-3084.

[36]. Narayanan, T. Small-Angle Scattering. In Structure from Diffraction Methods; Wiley Online Library: Hoboken, NJ, USA, 2014; pp. 259–324

[37]. An, Zhinan, et al. "Solid-solution CrCoCuFeNi high-entropy alloy thin films synthesized by sputter deposition." Materials Research Letters 3.4 (2015): 203-209.

[38]. Marshal, A., et al. "Combinatorial synthesis of high entropy alloys: Introduction of a novel, single phase, body-centered-cubic FeMnCoCrAl solid solution." Journal of Alloys and Compounds 691 (2017): 683-689.

[39]. Chao, Qi, et al. "Direct laser deposition cladding of AlxCoCrFeNi high entropy alloys on a high-temperature stainless steel." Surface and Coatings Technology 332 (2017): 440-451.

[40]. Csáki, Ioana, et al. "CoCrFeNiMo high entropy alloy produced by solid state processing." Key Engineering Materials. Vol. 750. Trans Tech Publications Ltd, 2017.

[41]. Huang, Yung-Chien, et al. "Nano-precipitates in severely deformed and low-temperature aged CoCrFeMnNi high-entropy alloy studied by synchrotron small-angle X-ray scattering." Intermetallics 105 (2019): 146-152.

اكتسبت الاغشية الرقيقة المصنعة من الانظمة السبائكية ذات الانتروبيا العالية في السنوات الاخيرة.هذا الاهتمام جاء نتيجة للخواص الهائلة التي تمتلكها هذه الانظمة السبائكية مثل مقاومة التاكل , الصلادة العالية و وخواص توصيل كهربائية عالية.هذه الخواص بدورها تعتمدعلى التركيب ,التركيب الكيميائي, عدم الانتظام, طبيعة السطح,والصفات الميتالورجية الاخرى زان تحديد هذه الخواص ولا سيما عند الاقتراب من المقياس

النانوي يتطلب تقنيات دقيقة مثل انحراف الاشعة السينيه مثل حيود الأشعة السينية (XRD) ، المجهر الإلكتروني الماسح (SEM) ، المجهر ذي المسبار الماسح (SPM) ، والأشعة السينية الطيفية الضوئية (XPS). يعتمد مبدأ XRD على التشتت المترابط المرن للطيف الأحادي اللون للأشعة السينية مع أقرب طول موجي للمسافة الشبكية في البناء البلوري. العديد من الطرق الهندسيةاستخدمت في توصيف XRD والتي إلى معلومات مختلفة. يعد THETA -2THETA مسحًا تقليديًا ووضعًا مشهورًا في الغالب ، حيث يتم استغلاله لإنتاج أنماط المراحل بكفاءة كافية يعتمد على اتجاه الطائرات الشبكية. بالنسبة للأغشية الرقيقة ، تؤدي زاوية السقوط الكبيرة إلى تداخل قمم المواد السائبة مع القمم الناتجة عن طبقة رقيقة ، ولهذا السبب ، تم اختراع تقنيات أخرى وتطويرها من خلال استغلال تشتت الأشعة السينية لحل هذه المشكلة مثل الزاوية الصغيرة التشتت (ساكس). تقدم هذه المراجعة خلفية موجزة عن XRD و SAXS وتطبيقاتهما.